Biogeosciences, 21, 3509–3522, 2024
https://doi.org/10.5194/bg-21-3509-2024

Biogeosciences Open Access EGU

Using eddy covariance observations to determine the carbon sequestration characteristics of subalpine forests in the Qinghai–Tibet Plateau

Niu Zhu[1,2,4], **Jinniu Wang**[1,2], **Dongliang Luo**[3], **Xufeng Wang**[3], **Cheng Shen**[1,2], **and Ning Wu**[1]

[1]Chengdu Institute of Biology, Chinese Academy of Sciences, Chengdu 610041, China
[2]Mangkang Ecological Monitoring Station, Tibet Ecological Security Barrier Ecological Monitoring Network, Qamdo 854500, China
[3]Northwest Institute of Eco-Environment and Resources, Chinese Academy of Sciences, Lanzhou 730000, China
[4]College of Resources and Environmental Sciences, Gansu Agricultural University, Lanzhou 730070, China

Correspondence: Jinniu Wang (wangjn@cib.ac.cn)

Received: 14 November 2023 – Discussion started: 28 November 2023
Revised: 28 May 2024 – Accepted: 12 June 2024 – Published: 6 August 2024

Abstract. Subalpine forests are a crucial component of the carbon cycling system in the Qinghai–Tibet Plateau (QTP). However, there are currently significant data gaps in the QTP, and it is essential to enhance continuous monitoring of forest carbon absorption processes in the future. This study investigates 2 years' carbon exchange dynamics of a subalpine forest on the QTP using an eddy covariance method. We first characterized the seasonal carbon dynamics of the subalpine forest, revealing the higher carbon dioxide (CO_2) exchange rates in summer and autumn and lower rates in winter and spring, and found that autumn is the peak period for carbon sequestration in this subalpine forest, with the maximum measured value of CO_2 absorption reaching $10.70\,\mu mol\,m^{-2}\,s^{-1}$. Subsequently, we examined the environmental factors influencing the carbon sequestration function. Principal component analysis (PCA) shows that photosynthetically active radiation (PAR) was the major environmental factor driving the net ecosystem exchange (NEE) of CO_2, significantly influencing forest carbon absorption, and the increase in relative humidity decreases the rate of carbon fixation. In addition, we explored NEE and its influencing factors at the regional scale and found that air temperature promotes carbon dioxide absorption (negative NEE values), while the average annual precipitation shows a minor effect on NEE. At the annual scale, the subalpine forest functions as a strong carbon sink, with an average NEE of -332 to $-351\,g\,C\,m^{-2}$ (from November 2020 to October 2022). Despite the challenges of climate change, forests remain robust carbon sinks with the highest carbon sequestration capacity in the QTP, with an average annual CO_2 absorption rate of $368\,g\,C\,m^{-2}$. This study provides valuable insights into the carbon cycling mechanism in subalpine ecosystems and the global carbon balance.

1 Introduction

Carbon dioxide (CO_2) is a prominent greenhouse gas, and its atmospheric concentration has reached an unprecedented high level in recent years. In May 2021, a recorded peak of 419 parts per million (ppm) was observed at the Mauna Loa Observatory in Hawaii (Stein, 2021). The global atmospheric CO_2 concentration is rapidly increasing at a rate of 2 to 3 ppm per year compared to pre-industrial levels, and the average global temperature had already risen by 1.1 °C by 2019 (World Meteorological Organization, 2019). Human activities are the primary catalyst behind the significant surge in atmospheric CO_2 concentrations (Schweizer et al., 2020). Among the six greenhouse gases specified in the Kyoto Protocol, CO_2 and CH_4 collectively contribute approximately 70 % to the global warming potential (Zhang et al., 2022). As atmospheric CO_2 concentrations continue to rise, global climate warming is gradually intensifying. Therefore, the Paris Agreement urges national governments to restrict

the increase in global average temperature to well below 2.0 °C above pre-industrial levels and to strive to limit it to 1.5 °C. The increasing atmospheric CO_2 levels will lead to irreversible ecological disasters. For instance, the concentration of CO_2 in the atmosphere is projected to double within approximately 50 years if global consumption of fossil fuels continues to rise at the current rate. Addressing the greenhouse effect caused by carbon dioxide and reducing its impact is a crucial challenge facing human society today. Reducing regional carbon emissions or per-capita carbon emissions is widely regarded as an effective approach to reducing carbon (Wang et al., 2023a). Nevertheless, countries around the world have already begun to commit to carbon reduction and carbon neutrality efforts. On 22 September 2020, during the 75th session of the United Nations General Assembly, the Chinese government announced "double carbon" goals, which aim to achieve carbon emission peaking by 2030 and carbon neutrality by 2060, in alignment with ecological conservation and sustainable development objectives (Yu, 2022). It is predicted that China's average forest carbon sequestration rate will reach $0.358\,\mathrm{Pg\,C\,yr^{-1}}$ by 2060 (Cai et al., 2022). This significant rate of carbon sequestration is expected to have a substantial impact on the environment and economy, providing negative feedback to global warming (Pan et al., 2011).

Currently, there are various methods available to accurately quantify the carbon sequestration potential of forests. Quantitative estimation of carbon sequestration potential still requires scientists to establish more in situ sites and generate comprehensive datasets to assess a wide range of areas. Initially, individuals' biomass measurements were used to estimate forest carbon sequestration capacity (Ebermayer, 1876). However, this method was time-consuming, labor-intensive, and prone to inaccuracies due to the omission of various variables during the calculation process. The development of modeling techniques has allowed for the use of simulation methods, forest management models, and land ecosystem–climate interaction models, such as the Ecological Assimilation of Land and Climate Observations (EALCO) model, which have been widely applied in this regard (Landsberg and Waring, 1997; Wang et al., 2001). Currently, remote sensing monitoring and the eddy covariance (EC) method are quite popular. Remote sensing techniques can be used to extract vegetation parameters (e.g., normalized difference vegetation index, NDVI) from multispectral bands and estimate the carbon sequestration of entire forests through regression analysis (Laurin et al., 2014). The eddy covariance method, allowing for continuous, long-term carbon flux calculation, provides fundamental data for model establishment and calibration. It has been widely applied across ecosystems, including urban areas, farmlands, grasslands, forests, and waterbodies (Konopka et al., 2021; Vote et al., 2015; Du et al., 2022a; Kondo et al., 2017; Li et al., 2022).

The forest ecosystem's net ecosystem exchange (NEE) of carbon dioxide is influenced by multiple environmental factors. Previous studies have shown that NEE is significantly influenced by air temperature (AT), photosynthetically active radiation (PAR), vapor pressure deficit (VPD), relative humidity (RH), and soil temperature (ST) (Liu et al., 2022). For instance, temperature variables, especially annual or seasonal average temperature variations, serve as the optimal single predictor for carbon flux, explaining variations in carbon flux between 19 % and 71 % (Banbury Morgan et al., 2021). PAR not only influences the absorption of carbon dioxide by the forest canopy but also affects the utilization of carbohydrates by roots due to its association with canopy processes and soil respiration (Baumgartner et al., 2020). Furthermore, research suggests that NEE is influenced by biotic factors such as NDVI and leaf area index (LAI) (Tang et al., 2022). Given the projected future global warming trends, forests play a highly significant role as vast carbon reservoirs that are worthy of attention. The Qinghai–Tibet Plateau (QTP) is the highest and largest plateau in the world, with an extensive area of alpine forests covering approximately $2.3 \times 10^5\,\mathrm{km^2}$, holding tremendous economic and ecological benefits. The southeastern region of the QTP boasts one of the world's highest-altitude subalpine forest ecosystems. Research indicates that the subalpine forest ecosystem in this area has a remarkable capacity to consume methane, reaching up to $5.06\,\mathrm{kg\,ha^{-1}\,yr^{-1}}$, playing a significant role in mitigating the impact of greenhouse gases (Qu et al., 2023). Since the 1960s, the QTP has experienced a faster warming rate than lowland areas, a phenomenon projected to intensify by the end of the 21st century (Li et al., 2019). Currently, the QTP is considered a weak carbon sink at the overall level, but the carbon source–sink dynamics vary among different ecosystems (Chen et al., 2022). For instance, most lakes in the QTP are currently characterized by supersaturated CO_2 levels (Cole et al., 1994). Mu et al. (2023) found that the thermokarst lakes serve as significant carbon sources through carbon flux measurements in 163 thermokarst lakes during the summer and autumn seasons. Wang et al. (2021) discovered that by comparing carbon fluxes in 10 high-mountain ecosystems with different grassland types, these ecosystems act as sinks for carbon dioxide. The alpine meadows in the eastern QTP have been identified as strong carbon sinks, with the highest annual average NEE recorded at $-284\,\mathrm{g\,C\,m^{-2}}$. Forest ecosystems play a crucial role in the southeastern edge of the QTP, providing important support for climate regulation and forestry-based economic activities. Moreover, recent predictive studies suggest that under both current and future climate scenarios, the forested area in this region is expected to expand further, with coniferous forests continuing to grow into higher altitudes (Liu et al., 2021). Due to the extensive presence of permafrost in the QTP, forest net primary productivity exhibits the most pronounced response to surface temperatures in the continuous permafrost zone over multiple years. Therefore, the changes in permafrost in the QTP

should not be overlooked, as they also have a significant impact on carbon absorption by forests (Mao et al., 2015). However, the QTP is a vast region with a widespread distribution of high-altitude and subalpine forests. Long-term monitoring is necessary to understand how these forests will respond to climate change. Furthermore, there is a significant data gap concerning the monitoring of carbon exchange capacity in the forests of the QTP, indicating the need for further data collection efforts. Based on this, we established a carbon flux monitoring site in the subalpine ecosystem of the Three Parallel Rivers region, which is located on the southeastern edge of the QTP and is renowned as a global hotspot for biodiversity (C. Y. Wang et al., 2022). Our research objectives are as follows:

1. to determine whether the subalpine forests in the Three Parallel Rivers region act as a carbon sink or source and quantify the annual uptake or release of carbon dioxide
2. to investigate the influences of the main environmental factors on the carbon exchange process in the subalpine forests and identify the factors with the greatest impact
3. to evaluate the carbon exchange capacity of subalpine forests in the QTP by comparing existing data with other ecosystems in the region.

This study provides a data foundation and background support for accurately estimating the carbon balance of forests in high-altitude areas and for model simulations in the future.

2 Materials and methods

2.1 Overview of the study site

The study site is located in the Hongla Mountain Yunnan Snub-nosed Monkey National Nature Reserve in Mangkang County, Tibet, China (29°17′10.78″ N, 98°41′27.45″ E), the core area of the watershed of the Three Parallel Rivers (Nujiang River, Lancang River, and Jinsha River). The elevation of the study site is 3755 m. The observation period was from November 2020 to October 2022. The study area experiences large diurnal temperature variations and dry conditions in winter, while the summers are warm and humid. The average daily sunshine duration exceeds 10 h, with an annual average temperature of 5° and an average annual precipitation of around 600 mm within a year (Niu et al., 2023). The main tree species in the area include *Picea likiangensis* var. *rubescens*, *Abies squamata*, *Sabina tibetica* Kom., and *Abies ernestii*. They are accompanied by the growth of some *Quercus aquifolioides*, *Rhododendron lapponicum*, and *Potentilla fruticosa* shrubs. The average height of the trees is around 30 m, and the forest is in a relatively active growth phase, reaching the state of a mature forest. The vegetation coverage ranges from 70 % to 80 %. The dominant soil type is yellow-brown soil. The mountainous terrain contributes to distinct vertical climate characteristics and significant variations in water and heat conditions, with numerous dry and hot river valleys, widespread canyons, and a clear impact from the southwestern and southeastern monsoons. The varying elevations give rise to diverse ecosystems, transitioning from alpine forests to mountain shrubs. Above 4000 m a.s.l., high alpine grasslands and meadows form a noticeable vegetation transition zone. The mountainous topography results in distinct vertical climate features and significant fluctuations in water and heat conditions, with precipitation showing a markedly uneven distribution throughout the study region (Zemin et al., 2023).

2.2 Eddy covariance system

The EC system is deployed at a 35 m high tower located at the study site. At the top of the tower, a 3-D wind velocity (WindMaster, Gill, UK) and an open-path infrared CO_2–H_2O analyzer (LI-7500DS, Li-Cor, USA) were installed to measure CO_2 flux. The instruments had a measurement frequency of 10 Hz. Additionally, micrometeorological sensors were placed at different heights on the tower, including sensors at 35 m for observing air temperature and humidity (HMP155A, Vaisala, Finland), sensors at −5 cm for soil temperature (TEROS 11, Li-Cor, USA), and sensors at 35 m for photosynthetically active radiation (LI-190R, Li-Cor, USA). All data were stored for 30 min in a SmartFlux 3 data logger (Li-Cor, USA) for future download.

2.3 Data processing and quality control

When considering only the turbulent transport of matter and energy in the vertical direction, the carbon dioxide flux (F_c) can be represented by the following equation (Yu and Sun, 2006; Monteith et al., 1994):

$$F_C = \overline{W'CO_2'}, \quad (1)$$

where W' is the vertical component of 3-D wind speed fluctuations ($m\,s^{-1}$), and CO_2' represents the fluctuations in the measured CO_2 mole concentration. A positive F_C indicates carbon emissions, while a negative value represents carbon uptake.

The acquired 10 Hz raw data were processed and corrected using EddyPro software (EddyPro 7.06, Li-Cor, USA). The calibration process involved outlier detection for flux data, lag elimination, coordinate rotation (Jia et al., 2020), ultrasonic temperature correction (Schotanus et al., 1983), frequency correction (Moncrieff et al., 1997), and Webb–Pearman–Leuning (WPL) correction (Leuning and King, 1992). After these controls, the integrity of the effective F_C raw data we obtained reached 92.95 %. We removed outliers caused by environmental disturbances such as power outages, rain, snow, and dust particles that interfered with the instrument. Due to the slope of the underlying surface being around 5°, we also corrected for non-uniform and non-flat

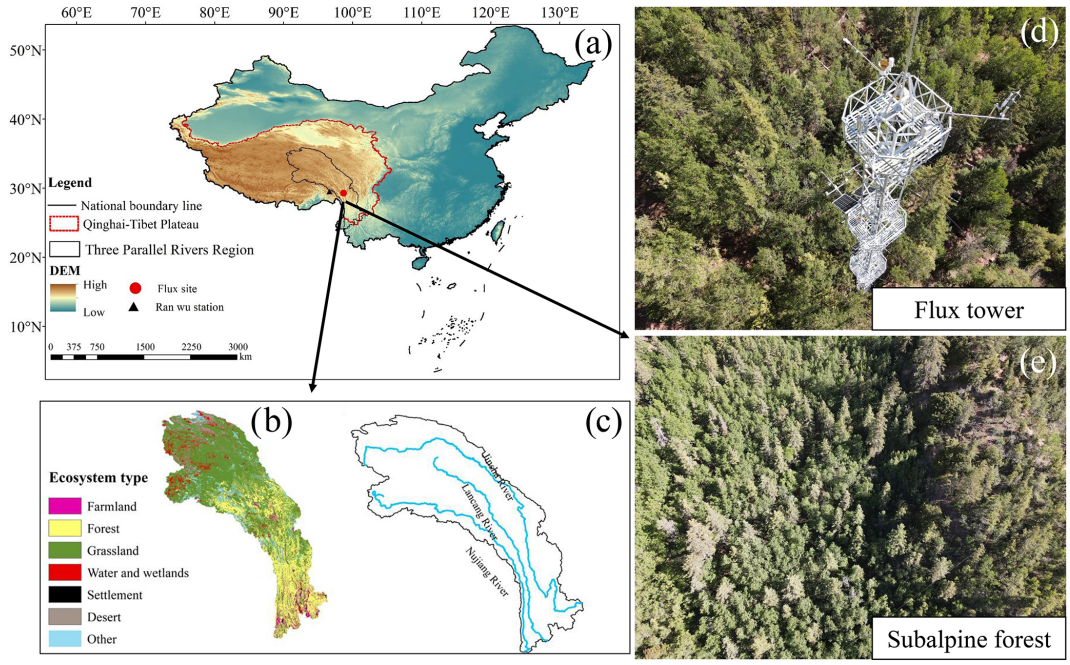

Figure 1. Publisher's remark: please note that the above figure contains disputed territories. Location of the flux site **(a)**. Ecosystem types **(b)** and main rivers **(c)** in the Three Parallel Rivers region. Flux tower **(d)** and forest top view **(e)**. The national boundary range in the figure was retrieved from http://bzdt.ch.mnr.gov.cn (last access: 10 May 2023), and elevation data and ecosystem type are from http://www.gscloud.cn (last access: 10 May 2023).

surfaces using EddyPro for double-coordinate rotation (Cao et al., 2019). As a result, we obtained half-hourly flux data with associated data quality indicators. To evaluate the turbulence steadiness, we employed the "0–1–2" quality assessment method, which classifies flux results into three quality levels: 0 for excellent data quality, 1 for moderate data quality, and 2 for low data quality (Mauder and Foken, 2015; Foken et al., 2005). We removed data points labeled with a quality level of 2. We further eliminated flux data with negative values during nighttime since plants do not perform photosynthesis at night. Additionally, we conducted spectral analysis to identify and remove data points with values significantly deviating from normal. Finally, friction velocities ($u*$) for each of the 2 years were determined separately using the moving-point method and deleted data recorded during nighttime when $u*$ was less than 0.28 and 0.39 $\mathrm{m\,s^{-1}}$ (Reichstein et al., 2005). After excluding outliers from the data, the data integrity was 72.67 %. Tovi software (Tovi, Li-Cor, USA) was used in the process.

When turbulence is weak, a portion of CO_2 is stored in the vegetation canopy and the atmosphere below the measurement height. At this time, the NEE is calculated as (Zhang et al., 2018)

$$\mathrm{NEE} = F_C + F_S, \tag{2}$$

where NEE represents the net ecosystem exchange of CO_2, F_C stands for the observed flux during a specific period, and F_S represents the CO_2 storage in the forest canopy. F_S is calculated as $(\Delta c/\Delta t)\,h$, where Δc is the difference in CO_2 concentration between two consecutive measurements, Δt is the time interval between two consecutive measurements, and h is 35 m.

We adopted the following formula as a gap-filling strategy for daytime NEE ($\mathrm{NEE_{day}}$) concerning PAR, aiming to address missing values during the daytime (Falge et al., 2001):

$$\mathrm{NEE_{day}} = \frac{\alpha \times \mathrm{PAR} \times P_{\max}}{\alpha \times \mathrm{PAR} + P_{\max}} - R_{\mathrm{day}}, \tag{3}$$

where α (μmol CO_2/μmol PAR) represents the apparent photosynthetic quantum efficiency, which characterizes the maximum efficiency of converting light energy during photosynthesis; PAR (μmol $\mathrm{m^{-2}\ s^{-1}}$) is the photosynthetically active radiation, a measure of the amount of light energy available for photosynthesis; $P_{\max}$ (μmol CO_2 $\mathrm{m^{-2}\ s^{-1}}$) is the apparent maximum photosynthetic rate, representing the maximum CO_2 uptake rate under optimal conditions; and R_{day} (μmol CO_2 $\mathrm{m^{-2}\ s^{-1}}$) is the daytime dark respiration rate, which denotes the rate of CO_2 release during daylight hours. We obtain α, $P_{\max}$, and R_{day} through the nonlinear fitting of the Michaelis–Menten model to the observed data.

During nighttime, the NEE is modeled using an exponential function of ecosystem respiration and soil temperature to fill in the missing values of NEE during the night ($\mathrm{NEE_{night}}$)

(Lloyd and Taylor, 1994; Kato et al., 2006):

$$NEE_{night} = a \times \exp(bt), \quad (4)$$

where a and b are estimated values for the exponential function used in modeling NEE_{night}, and t represents the soil temperature measured at the depth of 5 cm. Origin 2023 (OriginLab Corporation, USA) is the data processing software used for this analysis. For the missing data, interpolation was performed using Tovi software, allowing for data interpolation to fill in the gaps and ensuring a continuous dataset for further analysis (Reichstein et al., 2005). A total of 27.33 % of missing data were interpolated using Tovi after filtering, resulting in a flux dataset with complete data integrity.

In flux analysis, the significance of source area contributions cannot be overlooked. In this study, the peak distances of the 90 % flux contribution areas averaged over 2 years are 364.2 and 357.1 m. In terms of seasons, the average peak distances of the 90 % flux contribution areas for winter, spring, summer, and autumn over the 2 years are as follows: 353.9, 358.2, 350.05, and 344.34 m, respectively.

2.4 Flux partitioning

Ecosystem respiration (ER) is the sum of plant and heterotrophic respiration in an ecosystem and is obtained by adding the measured nighttime data to the extrapolated daytime data. Gross primary productivity (GPP) is the total amount of organic carbon fixed by green plants through photosynthesis per unit of time and per unit of area:

$$ER = R_{day} + R_{night}, \quad (5)$$

$$GPP = -NEE + ER. \quad (6)$$

Carbon use efficiency (CUE) is a crucial parameter that reflects the ability of an ecosystem to sequester carbon. It is defined as the ratio of net ecosystem productivity (NEP) to gross primary productivity. CUE can be expressed using the following equation:

$$CUE = \frac{NEP}{GPP} = \frac{-NEE}{GPP}. \quad (7)$$

To study the variation in ecosystem respiration rates with environmental factors, we considered the dependence of nocturnal ecosystem respiration on soil temperature (Pavelka et al., 2007; Mamkin et al., 2023):

$$Q_{10} = \exp(10 \times \alpha) \quad (8)$$

$$\ln(NEE_{night}) = \alpha \times T + \gamma, \quad (9)$$

where T is the soil temperature (°C), and γ is an empirical parameter of the equation.

To clarify the carbon sink potential of forests in the QTP and to compare it with other ecosystems, a search was conducted in two authoritative databases, the Web of Science and China National Knowledge Infrastructure, for research articles on the current utilization of EC systems in the QTP. A total of 82 research results were collected from 48 studies, and their annual average environmental factors, such as air temperature, precipitation, and altitude, were obtained.

3 Results

3.1 Daily changes in main environmental factors

During the observational period, the environmental conditions exhibited significant fluctuations. The winter and spring seasons were characterized by cold and dry conditions, while the summer and autumn seasons were warm and humid. The daily maximum AT recorded was 15.87° (on 15 June 2021), and the minimum temperature was −9.88° (on 17 January 2022), with a mean annual average of 5.5° over the 2 years. RH is averaged at 55.89 %, and VPD is averaged at 4.46 hPa. ST exhibited a similar trend to air temperature. The highest observed soil temperature was 13.53° (on 27 June 2021), while the minimum was −3.78° (on 18 January 2022), with an annual average of 6.11°. PAR is averaged at 447.24 mol m^{-2} s^{-1}.

3.2 Seasonal dynamics of NEE, ER, and GPP

The observations from the forest ecosystem indicate distinct diurnal and seasonal variations in NEE and GPP (Fig. 3). The NEE and GPP exhibit a pronounced U-shaped curve, with significant seasonal differences. Summer and autumn are characterized by peak carbon uptake, with the maximum NEE reaching 10.70 ± 5.19 µmol CO_2 m^{-2} s^{-1} (autumn, 12:30 Beijing time, UTC+8:00). During nighttime, the ecosystem generally releases carbon, while during favorable daytime meteorological conditions, it demonstrates a carbon uptake capacity. Peak carbon absorption of the forest ecosystem occurs from 12:00 to 15:00 (Beijing time, UTC+8:00). The daily carbon sequestration in summer and autumn is 1.5–3 h longer than in winter. The timing of maximum carbon sequestration capacity changes with each season. In winter, the transition from nighttime carbon release to daytime carbon uptake occurs around 08:30, which is approximately 1 h later than in summer. GPP characterizes the forest's carbon sequestration capacity, and since photosynthesis does not occur at night, GPP is zero during nighttime. The maximum daily total productivity is recorded at 14.76 ± 7.34 µmol CO_2 m^{-2} s^{-1} during the summer of the second year, with a standard deviation indicating greater variability in GPP and NEE during summer and autumn compared to winter and spring. Although diurnal variations in ER are relatively small, there are significant seasonal differences. During the night, when only respiration occurs, ER equals NEE. However, as photosynthesis becomes active during the day, ER gradually increases and stabilizes. The respiratory rate of the coniferous forest is the highest in autumn, being 8 times greater than in winter.

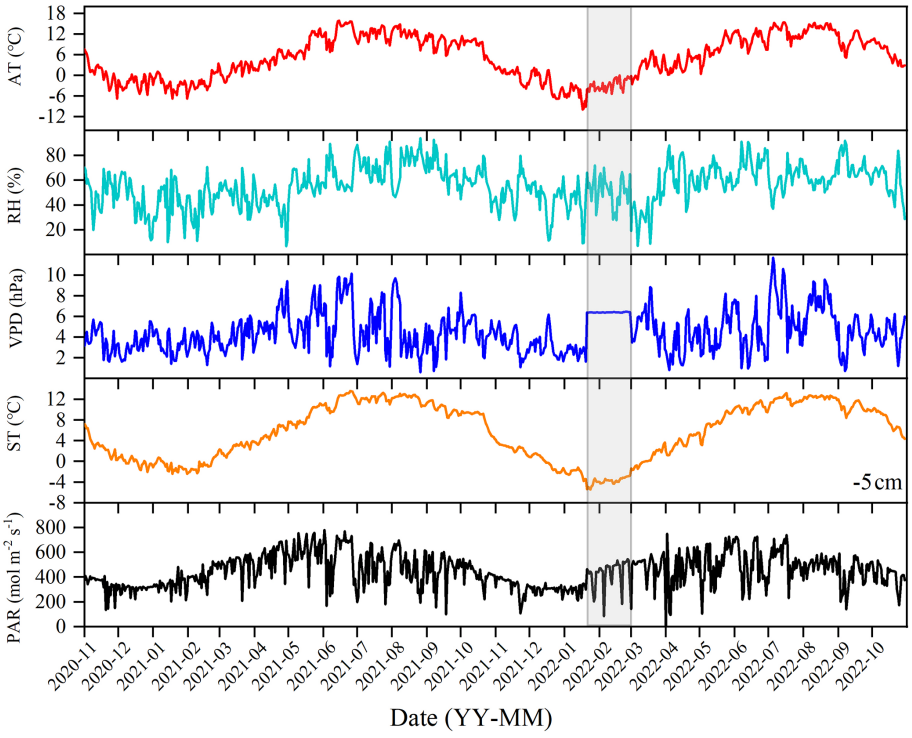

Figure 2. Daily values of main environmental factors: air temperature (AT), relative humidity (RH), vapor pressure deficit (VPD), soil temperature (ST), and photosynthetically active radiation (PAR). The data of the shaded part in the figure come from the Ranwu forest site (Fig. 1). Since there was no interpolated data source for VPD, the annual average was used instead.

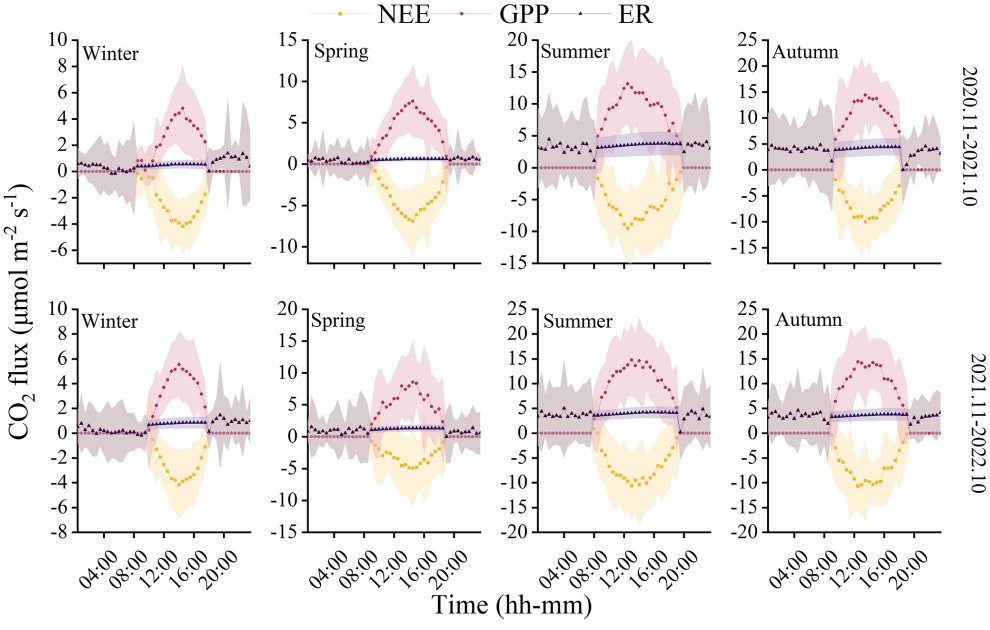

Figure 3. Monthly mean values of CO_2 fluxes.

3.3 Relationship between NEE and main environmental factors

Principal component analysis (PCA) of NEE and environmental factors (Fig. 4) indicates that the explanations for the first principal component (PC1) and the second principal component (PC2) are essentially the same between the 2 years. The total contributions of PC1 and PC2 are 87.7 % and 87.5 %, respectively, with PC1 accounting for 64.0 % and 64.6 % individually. The angle between photosynthetically active radiation (PAR) and PC1 is minimal, suggesting a strong correlation between PAR and PC1. Additionally, PAR and VPD contribute the most to PC1, while AT and RH contribute the most to PC2. The analysis results reveal a significant positive correlation between NEE and RH, while a significant negative correlation is observed with AT, VPD, and PAR. Increased RH is detrimental to forest carbon dioxide absorption. Excessively high relative humidity causes plant leaf stomata to close, reducing the amount of carbon dioxide available to the plant. This, in turn, leads to a decrease in the efficiency of carbon fixation through photosynthesis. Among these environmental factors, PAR plays a dominant role. Furthermore, Fig. 4 illustrates the relationships between environmental factors, showing a positive correlation between RH and TA and a negative correlation with VPD and APR. The indicators exhibit some seasonality, with notable differences between the winter–spring and summer–autumn seasons, indicating limited similarity between seasons.

3.4 Seasonal variation in NEE, GPP, and ER

NEE did not show significant interseasonal differences (Fig. 5). However, data distribution indicates that the variability in the NEE rate differs across different seasons, particularly between summer–autumn and winter–spring. The changes in GPP over the 2 years were similar, with significant differences observed between summer and winter ($P < 0.05$). The ER was higher during summer–autumn compared to winter–spring. The highest ecosystem respiration occurred in the first year during autumn, while in the second year, it was the highest during summer. Within the same year, summer and autumn exhibited significant differences ($P < 0.05$), while between the same seasons in different years, notable distinctions were not observed. This pattern is also reflected in GPP and NEE.

3.5 Changes in total NEE, GPP, ER, and CUE

The cumulative fluxes over the 2 years for the forest ecosystem are shown in Fig. 6. NEE indicates the net carbon sequestration in each month. The cumulative respiration reached its highest value of 361 g C m^{-2} in the summer of 2022. The total NEE, GPP, and ER for the first year were −332, 1121, and 788 g C m^{-2}, respectively, and −351, 1199, and 847 g C m^{-2} for the second year, respectively. CUE was higher during spring and lower during autumn, with a maximum value of 0.74 and a minimum value of 0.07. The average CUE over the 2 years was 0.40 and 0.35.

3.6 The carbon sequestration potential of the subalpine forests of the QTP

To clarify the carbon sequestration contribution of the subalpine forests found in the QTP, we compared these research results (Fig. 7). We found that ecosystems with high vegetation cover exhibited higher annual cumulative carbon sequestration. Among these ecosystems, the subalpine forests in the QTP showed the highest carbon sequestration potential, reaching an average of 368 g C m^{-2} yr^{-1}. The carbon sequestration potential of different ecosystems ranked as follows: forest > meadow > steppe > shrub. The average value for wetlands indicated that they are a significant source of CO_2, releasing 57 g C m^{-2} into the atmosphere annually. We also analyzed the influence of altitude, mean annual air temperature, and precipitation on NEE at these sites in the QTP. It has been observed that these sites cover a wide range of altitudes, ranging from 1977 to 4800 m. According to existing results, an increase in elevation may lead to a reduction in carbon uptake, while the range of mean annual temperature varies between −14.8 and 15.1°, and higher mean annual temperatures significantly increase carbon uptake. Forests exhibit the highest mean annual precipitation, averaging 827 mm, with mean annual precipitation having a relatively weak impact on NEE. These findings highlight the important role of subalpine forests in carbon sequestration in the QTP and provide insights into the factors that affect carbon exchange in the QTP, such as altitude, temperature, and precipitation.

4 Discussion

4.1 Main factors affecting the carbon sequestration function of subalpine forests

Climate change significantly affects the vegetation's carbon sequestration capacity, particularly at the seasonal scale due to phenological changes (Acosta-Hernández et al., 2020). In the short term, PAR, AT, RH, and VPD play important roles in regulating vegetation photosynthesis and, consequently, carbon uptake. For instance, PAR represents the portion of solar energy that can be utilized by plants and is an essential component in chloroplast reactions. PAR drives a nonlinear response of GPP to solar-induced fluorescence (SIF) across different seasons, resulting in a strong positive correlation between GPP and SIF (Wang et al., 2023b). VPD affects photosynthesis and transpiration of leaves, with stomata serving as tiny pores mediating carbon dioxide uptake. Research has demonstrated that excessive increases in VPD are detrimental to photosynthesis. For instance, a moderate increase in VPD significantly reduces photosynthetic effi-

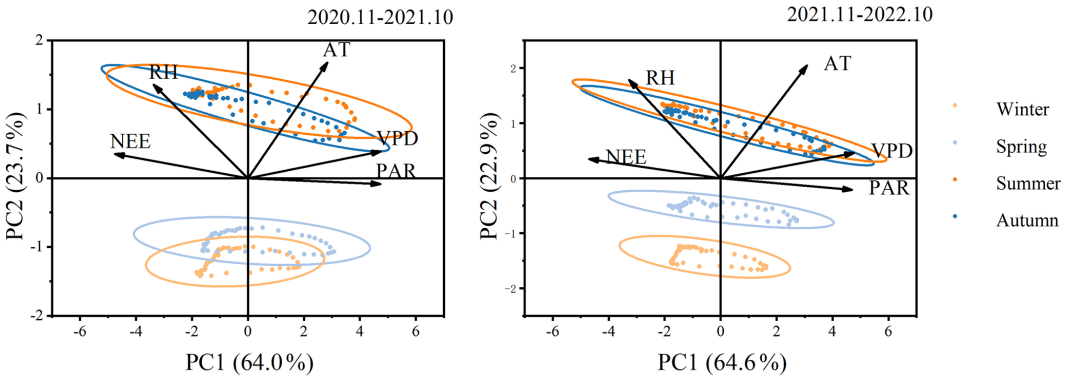

Figure 4. Principal component analysis of environmental factors and NEE.

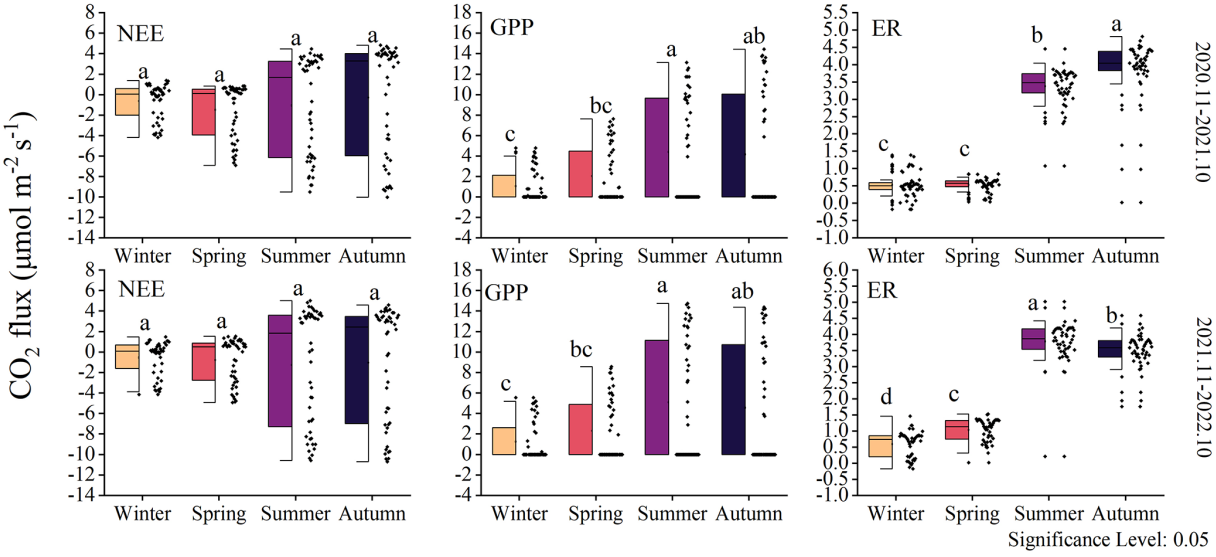

Figure 5. Seasonal variation in CO_2 fluxes in 2 years.

ciency under light fluctuations due to changes in RH and/or AT often accompanying fluctuations in light, and studies also indicate that the impact of VPD on sunlight utilization efficiency is primarily determined by RH rather than AT (Liu et al., 2024). In different seasons, the same influencing factors exhibit varying degrees of contribution to NEE. For example, during winter, when the climatic conditions are relatively harsh with low air temperature and humidity, the forest maintains a low level of carbon uptake. On longer timescales, such as annual and decadal variations, the inherent changes in forest NEE may be attributed to disturbances and recovery (Hayek et al., 2018). In this study, significant differences in ecosystem respiration were observed during summer and autumn in different years. Previous studies have suggested that due to leaf aging or water stress, the photosynthetic light use efficiency of the ecosystem peaks after spring leaf expansion and gradually declines (Wehr et al., 2016). This implies a peak in carbon exchange during summer, followed by higher productivity and ecosystem respiration in the following seasons. The variation in different years may be attributed to rainfall regulating the availability of natural resources such as water, biomass, litter, and soil nutrients (Schwinning and Sala, 2004). For instance, in temperate forests, when microbial biomass undergoes seasonal changes, microbial activity exhibits a seasonal lag in response to temperature variation, resulting in a seasonally delayed effect between litter heterotrophic respiration and temperature (Ataka et al., 2020). Whether such differences persist between different years on longer timescales remains to be demonstrated through more sustained and detailed research in the future. Ecosystem respiration sensitivity to temperature is represented by the Q_{10} coefficient. In this study, seasonal variations influenced the magnitude of Q_{10} (as shown in Fig. 8). The calculated Q_{10} for each season is as follows: 9.03, 2.22, 2.71, and 4.48. The winter season exhibited the highest sensitivity of forest ecosystem respiration to temperature, indicating that respiration rates in winter are more responsive to changes in temperature compared to other seasons. The main reason for

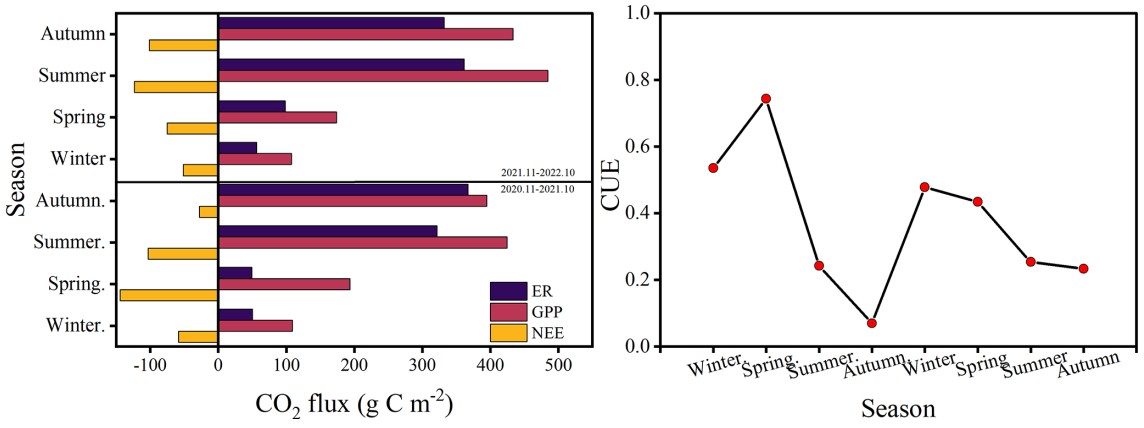

Figure 6. Change in total carbon flux and carbon use efficiency.

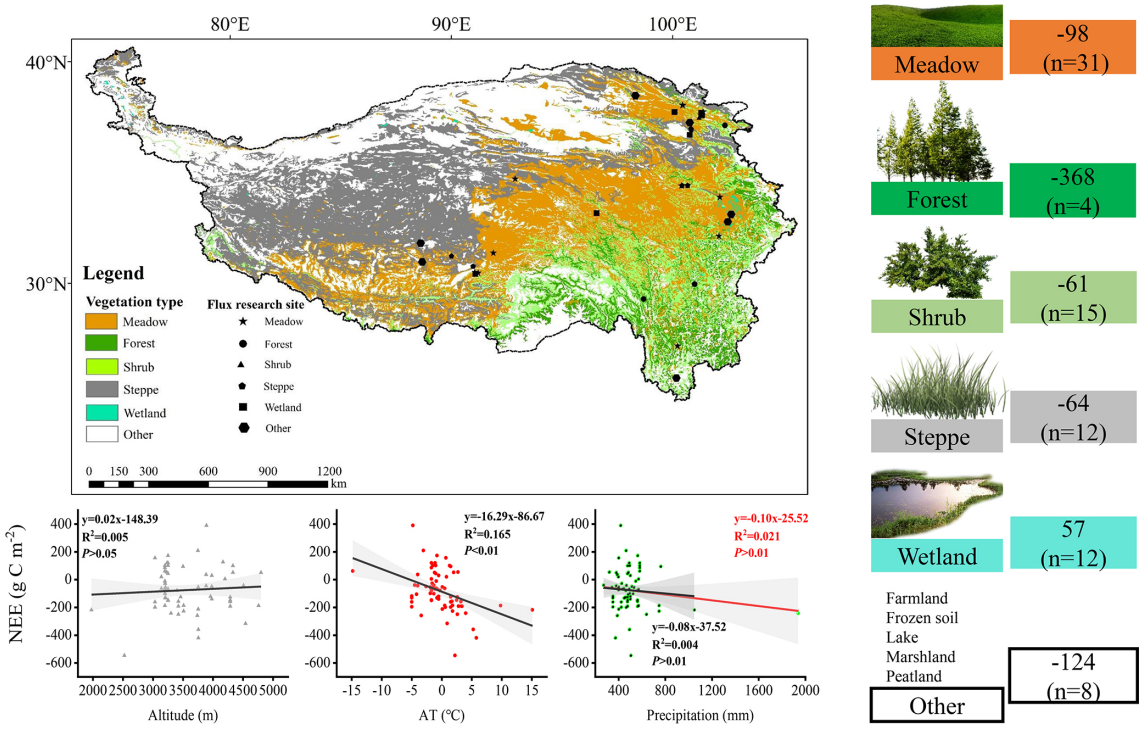

Figure 7. Carbon exchange potential of different ecosystems in the Qinghai–Tibet Plateau.

such differences is that ecosystem respiration consists of heterotrophic respiration and autotrophic respiration, which are typically governed by different factors (Edwards, 1975). For instance, the high activity of soil microbes contributes to heterotrophic respiration, a process dominated by soil temperature and moisture conditions, which are severely restricted during the cold and dry conditions of winter (Falge et al., 2002). Simultaneously, due to the changing relative roles of growth and maintenance respiration, the allocation of autotrophic respiration varies seasonally. In winter, soil CO_2 emissions constitute a significant portion of ecosystem CO_2 emissions, and in some boreal forests, the ratio between the two can reach 0.6 or even higher (Davidson et al., 2006). In winter, under the frequent coverage of snow, cold-adapted microorganisms thriving in a relatively narrow sub-zero temperature range engage in respiration and exhibit relatively high sensitivity to warming or cooling beyond this range (Monson et al., 2006). The seasonal patterns of the Q_{10} value are jointly determined by the variation in the ratio of soil respiration to ecosystem respiration, reflecting these seasonal changes.

Our integrated analysis (as shown in Fig. 7) reveals that despite the high elevation of the Third Pole, the topographic factor of elevation does not have a significant impact on car-

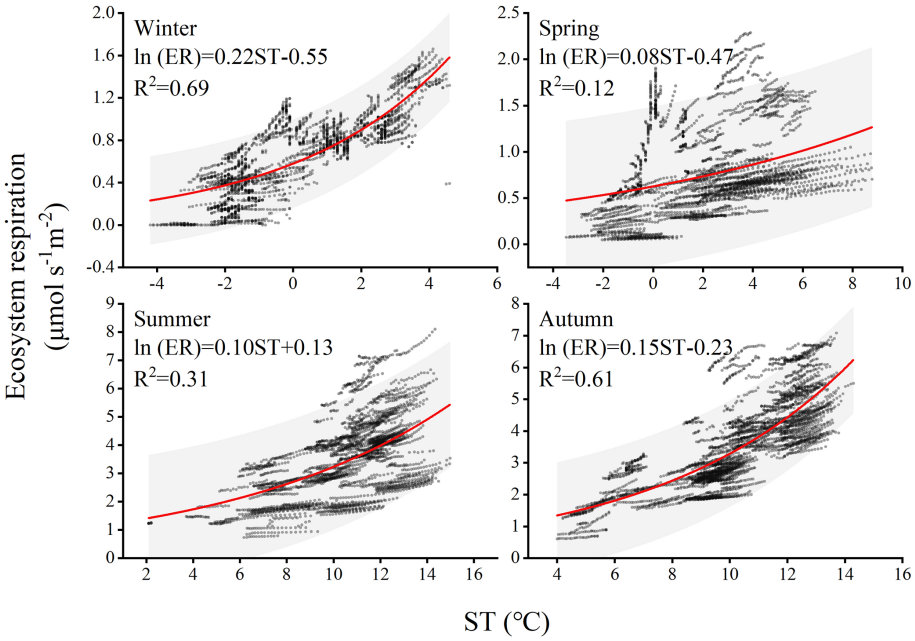

Figure 8. Relationship between NEE at night and soil temperature in different seasons.

bon uptake. Instead, NEE gradually increases with a steep rise in elevation. Research conducted by Wang et al. (2023c) has indicated that mean annual average temperature and precipitation are the main driving factors of interannual variations in NEE in alpine meadows and alpine steppes. Decreased precipitation resulted in a transition into carbon sources in some regions with high precipitation-dependent alpine grasslands. It is worth noting that, among all data collection sites, alpine wetlands show an average carbon source trend. Due to prolonged flooding and low temperatures, microbial activity in alpine wetlands is hindered, and the accumulation of organic carbon from plant litter decomposition is substantial. As a result, approximately 57 g C m^{-2} is emitted into the atmosphere annually. Previous studies have indicated that NEE in alpine wetlands is increasing with global warming (Yasin et al., 2022).

4.2 Sustained carbon sequestration of subalpine forests

Subalpine forests are integral components of global alpine ecosystems and play crucial roles in the global carbon cycle. Our study on subalpine forests demonstrates a continuous absorption of carbon dioxide even during winter, which aligns well with measurements taken in the vicinity of Mount Fuji in Japan (Mizoguchi et al., 2012). The age of subalpine forests is a crucial factor influencing sustained carbon sequestration. Based on NPP simulations of natural subalpine forests in the Northern Rockies, Carey (2001) found that aboveground net primary productivity reaches its maximum after approximately 250 years, followed by a decline. This challenges the previous view that forests older than 100 years are generally considered to be unimportant carbon sinks. Compared to the (mature) forest of Mount Gongga in the QTP (e.g., Zhang et al., 2018), the subalpine forest in this study exhibits a stronger carbon sequestration capacity. However, its carbon sequestration ability is slightly weaker than that of the Qilian Mountain high-mountain forests (approximately 60–70 years old) in the QTP (Zhang et al., 2018; Du et al., 2022b). Although existing flux monitoring results of high-altitude forests in the QTP indicate that these forest ecosystems act as carbon sinks, it is important to consider that globally there are still many cold regions with coniferous forests serving as carbon sources. For example, continuous CO_2 flux monitoring from native boreal forests in Sweden for over 10 years indicates that they are a net carbon source, which is attributed to the contribution of woody debris to ER due to disturbances such as extreme weather events, fires, insect infestations, and pathogen attacks (Hadden and Grelle, 2017). In the summer of 2018, Europe experienced a heat wave that affected the carbon cycling in forests. The mixed coniferous–deciduous forest in southern Estonia, under the influence of the heat wave, transitioned from a net carbon sink to a net carbon source in 2018 (Krasnova et al., 2022). Particular attention should be paid to the long-term monitoring in high-altitude environments of the impact of disturbances on forest carbon sequestration capacity. Our study has shown that forests in the QTP have the strongest carbon sink capacity, indicating that alpine forests will have an important sustained effect on carbon reduction in the QTP in the context of future climate change, but whether this sustained effect will be longer than other ecosystems is still unknown. However, a modeling experiment in a large semi-arid area of

California predicted that grasslands are more resilient carbon sinks than forests in responding to climate change in the 21st century (Dass et al., 2018). In terms of carbon sequestration rate, forests in the QTP were significantly stronger than other ecosystems, followed by grasslands, while alpine deserts and alpine grasslands in the northwestern and southern regions were the main carbon sources (Wu et al., 2022). Forests are mostly distributed in the southeastern margin of the QTP and the mid-altitude area near 3000 m in the Sichuan–Tibet alpine gorge area, with an area of 19.3×10^4 km^2 (Z. Y. Wang et al., 2022b). Based on the average value of current carbon flux monitoring, the forest in the QTP will absorb about 71×10^6 Mg C yr^{-1}.

5 Conclusions

This study explores the carbon sequestration function, seasonal variations, and climate drivers of subalpine forests in the QTP. Over the observational period, we synchronously monitored ecosystem carbon exchange and primary environmental factors using an eddy covariance system. The research reveals that the subalpine forest acts as a carbon sink. Over the 2 years, the total NEE, GPP, and ER were −332, 1121, and 788 g C m^{-2} in the first year and −351, 1199, and 847 g C m^{-2} in the second year, respectively. Photosynthetically active radiation was identified as the primary control of NEE. Relative humidity is negatively correlated with NEE, and its increase is not conducive to carbon sink. NEE reached its peak in autumn. Combining results from other eddy covariance sites on the QTP, this study highlights that forests have the highest carbon sequestration potential, reaching 368 g C m^{-2} annually, followed by meadows (−98 g C m^{-2}), steppes (−64 g C m^{-2}), and shrubs (−61 g C m^{-2}). In contrast, wetlands were identified as a significant source of carbon dioxide (57 g C m^{-2}). Despite the challenges posed by climate change, the subalpine forests in the QTP retain substantial carbon sequestration potential. Strengthening conservation and management efforts for subalpine forests is crucial to ensure their continued and significant carbon sequestration function in the future. Overall, this research underscores the vital role of subalpine forests in the QTP as essential carbon sink regions, playing a critical role in the context of global climate change.

Data availability. The data are available from the authors on request.

Supplement. The supplement related to this article is available online at: https://doi.org/10.5194/bg-21-3509-2024-supplement.

Author contributions. NZ: conceptualization, study design, data analyses, visualization, writing (original draft). JW: study design, writing (reviewing and editing), supervision, project administration, funding acquisition. DL and XW: writing (reviewing and editing). CS and NW: resources, data curation, supervision. All authors approved the final paper.

Competing interests. The contact author has declared that none of the authors has any competing interests.

Disclaimer. Publisher's note: Copernicus Publications remains neutral with regard to jurisdictional claims made in the text, published maps, institutional affiliations, or any other geographical representation in this paper. While Copernicus Publications makes every effort to include appropriate place names, the final responsibility lies with the authors.

Acknowledgements. We thank Neha Bisht for her substantial comments and language revision on an earlier version of the paper.

Financial support. This research has been supported by the CAS Light of West China program (2021XBZG-XBQNXZ-A-007); the National Natural Science Foundation of China (grant no. 31971436); and the State Key Laboratory of Cryospheric Sciences, Chinese Academy of Sciences (grant no. SKLCS-OP-2021-06).

Review statement. This paper was edited by Paul Stoy and reviewed by Haijun Peng and one anonymous referee.

References

Acosta-Hernández, A. C., Padilla-Martínez, J. R., Hernández-Díaz, J. C., Prieto-Ruiz, J. A., Goche-Telles, J. R., Nájera-Luna, J. A., and Pompa-García, M.: Influence of Climate on Carbon Sequestration in Conifers Growing under Contrasting Hydro-Climatic Conditions, Forests, 11, 1134, https://doi.org/10.3390/f11111134, 2020.

Ataka, M., Kominami, Y., Sato, K., and Yoshimura, K.: Microbial Biomass Drives Seasonal Hysteresis in Litter Heterotrophic Respiration in Relation to Temperature in a Warm-Temperate Forest, J. Geophys. Res.-Biogeo., 125, e2020JG005729, https://doi.org/10.1029/2020JG005729, 2020.

Banbury Morgan, R., Herrmann, V., Kunert, N., Bond-Lamberty, B., Muller-Landau, H. C., and Anderson-Teixeira, K. J.: Global patterns of forest autotrophic carbon fluxes, Glob. Change Biol., 27, 2840–2855, https://doi.org/10.1111/gcb.15574, 2021.

Baumgartner, S., Barthel, M., Drake, T. W., Bauters, M., Makelele, I. A., Mugula, J. K., Summerauer, L., Gallarotti, N., Cizungu Ntaboba, L., Van Oost, K., Boeckx, P., Doetterl, S., Werner, R. A., and Six, J.: Seasonality, drivers, and isotopic composition of soil CO_2 fluxes from tropical forests of the Congo Basin, Biogeosciences, 17, 6207–6218, https://doi.org/10.5194/bg-17-6207-2020, 2020.

Cai, W., He, N., Li, M., Xu, L., Wang, L., Zhu, J., Zeng, N., Yan, P., Si, G., and Zhang, X.: Carbon sequestration of Chinese forests from 2010 to 2060: Spatiotemporal dynamics and its regulatory strategies, Science Bull., 67, 836–843, https://doi.org/10.1016/j.scib.2021.12.012, 2022.

Cao, S., Cao, G., Chen, K., Han, G., Liu, Y., Yang, Y., and Li, X.: Characteristics of CO_2, water vapor, and energy exchanges at a headwater wetland ecosystem of the Qinghai Lake, Can. J. Soil Sci., 99, 227–243, https://doi.org/10.1139/cjss-2018-0104, 2019.

Carey, E. V., Sala, A., Keane, R., and Callaway, R. M.: Are old forests underestimated as global carbon sinks?, Glob. Change Biol., 7, 339–344, https://doi.org/10.1046/j.1365-2486.2001.00418.x, 2001.

Chen, H., Ju, P. J., Zhu, Q., Xu, X. L., Wu, N., Gao, Y. H., Feng, X. J., Tian, J. Q., Niu, S. L., Zhang, Y. J., Peng, C. H., and Wang, Y. F.: Carbon and nitrogen cycling on the Qinghai-Tibetan Plateau, Nature Reviews Earth & Environment, 3, 701–716, https://doi.org/10.1038/s43017-022-00344-2, 2022.

Cole, J. J., Caraco, N. F., Kling, G. W., and Kratz, T. K.: Carbon dioxide supersaturation in the surface waters of lakes, Science, 265, 1568–1570, https://doi.org/10.1126/science.265.5178.1568, 1994.

Dass, P., Houlton, B. Z., Wang, Y., and Warlind, D.: Grasslands may be more reliable carbon sinks than forests in California, Environ. Res. Lett., 13, 074027, https://doi.org/10.1088/1748-9326/aacb39, 2018.

Davidson, E. A., Richardson, A. D., Savage, K. E., and Hollinger, D. Y.: A distinct seasonal pattern of the ratio of soil respiration to total ecosystem respiration in a spruce-dominated forest, Glob. Change Biol., 12, 230–239, https://doi.org/10.1111/j.1365-2486.2005.01062.x, 2006.

Du, C., Zhou, G., and Gao, Y.: Grazing exclusion alters carbon flux of alpine meadow in the Tibetan Plateau, Agr. Forest Meteorol., 314, 108774, https://doi.org/10.1016/j.agrformet.2021.108774, 2022a.

Du, Y., Pei, W., Zhou, H., Li, J., Wang, Y., and Chen, K.: Net ecosystem exchange of carbon dioxide fluxes and its driving mechanism in the forests on the Tibetan Plateau, Biochem. Syst. Ecol., 103, 104451, https://doi.org/10.1016/j.bse.2022.104451, 2022b.

Ebermayer, E.: Die gesammte Lehre der Waldstreu mit Rücksicht auf die chemische Statik des Waldbaues: unter Zugrundlegung der in den Königl. Staatsforsten Bayerns angestellten Untersuchungen, ISBN 3642896340, Springer, 1876.

Edwards, N. T.: Effects of Temperature and Moisture on Carbon Dioxide Evolution in a Mixed Deciduous Forest Floor, Soil Sci. Soc. Am. J., 39, 361–365, https://doi.org/10.2136/sssaj1975.03615995003900020034x, 1975.

Falge, E., Baldocchi, D., Olson, R., Anthoni, P., Aubinet, M., Bernhofer, C., Burba, G., Ceulemans, R., Clement, R., Dolman, H., Granier, A., Gross, P., Grünwald, T., Hollinger, D., Jensen, N.-O., Katul, G., Keronen, P., Kowalski, A., Lai, C. T., Law, B. E., Meyers, T., Moncrieff, J., Moors, E., Munger, J. W., Pilegaard, K., Rannik, Ü., Rebmann, C., Suyker, A., Tenhunen, J., Tu, K., Verma, S., Vesala, T., Wilson, K., and Wofsy, S.: Gap filling strategies for defensible annual sums of net ecosystem exchange, Agr. Forest Meteorol., 107, 43–69, https://doi.org/10.1016/S0168-1923(00)00225-2, 2001.

Falge, E., Baldocchi, D., Tenhunen, J., Aubinet, M., Bakwin, P., Berbigier, P., Bernhofer, C., Burba, G., Clement, R., Davis, K. J., Elbers, J. A., Goldstein, A. H., Grelle, A., Granier, A., Guðmundsson, J., Hollinger, D., Kowalski, A. S., Katul, G., Law, B. E., Malhi, Y., Meyers, T., Monson, R. K., Munger, J. W., Oechel, W., Paw U, K. T., Pilegaard, K., Rannik, Ü., Rebmann, C., Suyker, A., Valentini, R., Wilson, K., and Wofsy, S.: Seasonality of ecosystem respiration and gross primary production as derived from FLUXNET measurements, Agr. Forest Meteorol., 113, 53–74, https://doi.org/10.1016/S0168-1923(02)00102-8, 2002.

Foken, T., Göockede, M., Mauder, M., Mahrt, L., Amiro, B., and Munger, W.: Post-Field Data Quality Control, in: Handbook of Micrometeorology: A Guide for Surface Flux Measurement and Analysis, edited by: Lee, X., Massman, W., and Law, B., Springer Netherlands, Dordrecht, 181–208, https://doi.org/10.1007/1-4020-2265-4_9, 2005.

Hadden, D. and Grelle, A.: Net CO_2 emissions from a primary boreo-nemoral forest over a 10year period, Forest Ecol. Manage., 398, 164–173, https://doi.org/10.1016/j.foreco.2017.05.008, 2017.

Hayek, M. N., Longo, M., Wu, J., Smith, M. N., Restrepo-Coupe, N., Tapajós, R., da Silva, R., Fitzjarrald, D. R., Camargo, P. B., Hutyra, L. R., Alves, L. F., Daube, B., Munger, J. W., Wiedemann, K. T., Saleska, S. R., and Wofsy, S. C.: Carbon exchange in an Amazon forest: from hours to years, Biogeosciences, 15, 4833–4848, https://doi.org/10.5194/bg-15-4833-2018, 2018.

Jia, X., Mu, Y., Zha, T., Wang, B., Qin, S., and Tian, Y.: Seasonal and interannual variations in ecosystem respiration in relation to temperature, moisture, and productivity in a temperate semi-arid shrubland, Sci. Total Environ., 709, 136210, https://doi.org/10.1016/j.scitotenv.2019.136210, 2020.

Kato, T., Tang, Y., Gu, S., Hirota, M., Du, M., Li, Y., and Zhao, X.: Temperature and biomass influences on interannual changes in CO_2 exchange in an alpine meadow on the Qinghai-Tibetan Plateau, Glob. Change Biol., 12, 1285–1298, https://doi.org/10.1111/j.1365-2486.2006.01153.x, 2006.

Kondo, M., Saitoh, T. M., Sato, H., and Ichii, K.: Comprehensive synthesis of spatial variability in carbon flux across monsoon Asian forests, Agr. Forest Meteorol., 232, 623–634, https://doi.org/10.1016/j.agrformet.2016.10.020, 2017.

Konopka, J., Heusinger, J., and Weber, S.: Extensive Urban Green Roof Shows Consistent Annual Net Uptake of Carbon as Documented by 5 Years of Eddy-Covariance Flux Measurements, J. Geophys. Res.-Biogeo., 126, e2020JG005879, https://doi.org/10.1029/2020JG005879, 2021.

Krasnova, A., Mander, Ü., Noe, S. M., Uri, V., Krasnov, D., and Soosaar, K.: Hemiboreal forests' CO_2 fluxes response to the European 2018 heatwave, Agr. Forest Meteorol., 323, 109042, https://doi.org/10.1016/j.agrformet.2022.109042, 2022.

Landsberg, J. and Waring, R.: A generalised model of forest productivity using simplified concepts of radiation-use efficiency, carbon balance and partitioning, Forest Ecol. Manage., 95, 209–228, https://doi.org/10.1016/S0378-1127(97)00026-1, 1997.

Laurin, G. V., Chen, Q., Lindsell, J. A., Coomes, D. A., Del Frate, F., Guerriero, L., Pirotti, F., and Valentini, R.: Above ground biomass estimation in an African tropical forest with lidar and hyperspectral data, ISPRS J. Photogramm., 89, 49–58, https://doi.org/10.1016/j.isprsjprs.2014.01.001, 2014.

Leuning, R. and King, K. M.: Comparison of eddy-covariance measurements of CO_2 fluxes by open- and closed-path CO_2 analysers, Bound.-Lay. Meteorol., 59, 297–311, https://doi.org/10.1007/BF00119818, 1992.

Li, L., Zhang, Y., Wu, J., Li, S., Zhang, B., Zu, J., Zhang, H., Ding, M., and Paudel, B.: Increasing sensitivity of alpine grasslands to climate variability along an elevational gradient on the Qinghai-Tibet Plateau, Sci. Total Environ., 678, 21–29, https://doi.org/10.1016/j.scitotenv.2019.04.399, 2019.

Li, X. Y., Shi, F. Z., Ma, Y. J., Zhao, S. J., and Wei, J. Q.: Significant winter CO_2 uptake by saline lakes on the Qinghai-Tibet Plateau, Glob. Change Biol., 28, 2041–2052, https://doi.org/10.1111/gcb.16054, 2022.

Liu, C., Wu, Z., Hu, Z., Yin, N., Islam, A. T., and Wei, Z.: Characteristics and influencing factors of carbon fluxes in winter wheat fields under elevated CO_2 concentration, Environ. Pollut., 307, 119480, https://doi.org/10.1016/j.envpol.2022.119480, 2022.

Liu, J., Zou, H.-X., Bachelot, B., Dong, T., Zhu, Z., Liao, Y., Plenković-Moraj, A., and Wu, Y.: Predicting the responses of subalpine forest landscape dynamics to climate change on the eastern Tibetan Plateau, Glob. Change Biol., 27, 4352–4366, https://doi.org/10.1111/gcb.15727, 2021.

Liu, N.-Y., Yang, Q.-Y., Wang, J.-H., Zhang, S.-B., Yang, Y.-J., and Huang, W.: Differential Effects of Increasing Vapor Pressure Deficit on Photosynthesis at Steady State and Fluctuating Light, J. Plant Growth Regul., 43, 2329–2339, https://doi.org/10.1007/s00344-024-11268-0, 2024.

Lloyd, J. and Taylor, J. A.: On the temperature dependence of soil respiration, Funct. Ecol., 8, 315–323, https://doi.org/10.2307/2389824, 1994.

Mamkin, V., Avilov, V., Ivanov, D., Varlagin, A., and Kurbatova, J.: Interannual variability in the ecosystem CO_2 fluxes at a paludified spruce forest and ombrotrophic bog in the southern taiga, Atmos. Chem. Phys., 23, 2273–2291, https://doi.org/10.5194/acp-23-2273-2023, 2023.

Mao, D., Luo, L., Wang, Z., Zhang, C., and Ren, C.: Variations in net primary productivity and its relationships with warming climate in the permafrost zone of the Tibetan Plateau, J. Geogr. Sci., 25, 967–977, https://doi.org/10.1007/s11442-015-1213-8, 2015.

Mauder, M. and Foken, T.: Documentation and Instruction Manual of the Eddy-Covariance Software Package TK3, Arbeitsergebnisse, Universität Bayreuth, Abt. Mikrometeorologie, 62 pp., 2015.

Mizoguchi, Y., Ohtani, Y., Takanashi, S., Iwata, H., Yasuda, Y., and Nakai, Y.: Seasonal and interannual variation in net ecosystem production of an evergreen needleleaf forest in Japan, J. Forest Res., 17, 283–295, https://doi.org/10.1007/s10310-011-0307-0, 2012.

Moncrieff, J. B., Massheder, J. M., de Bruin, H., Elbers, J., Friborg, T., Heusinkveld, B., Kabat, P., Scott, S., Soegaard, H., and Verhoef, A.: A system to measure surface fluxes of momentum, sensible heat, water vapour and carbon dioxide, J. Hydrol., 188–189, 589–611, https://doi.org/10.1016/S0022-1694(96)03194-0, 1997.

Monson, R. K., Lipson, D. L., Burns, S. P., Turnipseed, A. A., Delany, A. C., Williams, M. W., and Schmidt, S. K.: Winter forest soil respiration controlled by climate and microbial community composition, Nature, 439, 711–714, https://doi.org/10.1038/nature04555, 2006.

Monteith, J. L., Unsworth, M. H., and Webb, A.: Principles of environmental physics, Q. J. Roy. Meteor. Soc., 120, 1699, https://doi.org/10.1002/qj.49712052015, 1994.

Mu, C., Mu, M., Wu, X., Jia, L., Fan, C., Peng, X., Ping, C. l., Wu, Q., Xiao, C., and Liu, J.: High carbon emissions from thermokarst lakes and their determinants in the Tibet Plateau, Glob. Change Biol., 29, 2732–2745, https://doi.org/10.1111/gcb.16658 2023.

Niu, Z., Jinniu, W., Xufeng, W., Dongliang, L., Cheng, S., and Aihong, G.: Net ecosystem CO_2 exchange and its influencing factors in non-growing season at a sub-alpine forest in the core Three Parallel Rivers region, Acta Ecologica Sinica, 43, 5967–5979, https://www.ecologica.cn/stxb/article/abstract/stxb202204020841 (last access: 1 August 2024), 2023 (in Chinese).

Pan, Y., Birdsey, R. A., Fang, J., Houghton, R., Kauppi, P. E., Kurz, W. A., Phillips, O. L., Shvidenko, A., Lewis, S. L., and Canadell, J. G.: A large and persistent carbon sink in the world's forests, Science, 333, 988–993, https://doi.org/10.1126/science.1201609, 2011.

Pavelka, M., Acosta, M., Marek, M. V., Kutsch, W., and Janous, D.: Dependence of the Q10 values on the depth of the soil temperature measuring point, Plant Soil, 292, 171–179, https://doi.org/10.1007/s11104-007-9213-9, 2007.

Qu, S., Xu, R., Yu, J., and Borjigidai, A.: Extensive atmospheric methane consumption by alpine forests on Tibetan Plateau, Agr. Forest Meteorol., 339, 109589, https://doi.org/10.1016/j.agrformet.2023.109589, 2023.

Reichstein, M., Falge, E., Baldocchi, D., Papale, D., Aubinet, M., Berbigier, P., Bernhofer, C., Buchmann, N., Gilmanov, T., Granier, A., Grünwald, T., Havránková, K., Ilvesniemi, H., Janous, D., Knohl, A., Laurila, T., Lohila, A., Loustau, D., Matteucci, G., Meyers, T., Miglietta, F., Ourcival, J.-M., Pumpanen, J., Rambal, S., Rotenberg, E., Sanz, M., Tenhunen, J., Seufert, G., Vaccari, F., Vesala, T., Yakir, D., and Valentini, R.: On the separation of net ecosystem exchange into assimilation and ecosystem respiration: review and improved algorithm, Glob. Change Biol., 11, 1424–1439, https://doi.org/10.1111/j.1365-2486.2005.001002.x, 2005.

Schotanus, P., Nieuwstadt, F. T. M., and De Bruin, H. A. R.: Temperature measurement with a sonic anemometer and its application to heat and moisture fluxes, Bound.-Lay. Meteorol., 26, 81–93, https://doi.org/10.1007/BF00164332, 1983.

Schweizer, V. J., Ebi, K. L., van Vuuren, D. P., Jacoby, H. D., Riahi, K., Strefler, J., Takahashi, K., van Ruijven, B. J., and Weyant, J. P.: Integrated Climate-Change Assessment Scenarios and Carbon Dioxide Removal, One Earth, 3, 166–172, https://doi.org/10.1016/j.oneear.2020.08.001, 2020.

Schwinning, S. and Sala, O. E.: Hierarchy of responses to resource pulses in arid and semi-arid ecosystems, Oecologia, 141, 211–220, https://doi.org/10.1007/s00442-004-1520-8, 2004.

Stein, T.: Carbon dioxide peaks near 420 parts per million at Mauna Loa observatory, NOAA Research, June, 7, https://research.noaa.gov/2021/06/07 (last access: 5 March 2024), 2021.

Tang, X., Xiao, J., Ma, M., Yang, H., Li, X., Ding, Z., Yu, P., Zhang, Y., Wu, C., Huang, J., and Thompson, J. R.: Satellite evidence for China's leading role in restoring vegetation productivity over global karst ecosystems, Forest Ecol. Manage., 507, 120000, https://doi.org/10.1016/j.foreco.2021.120000, 2022.

Vote, C., Hall, A., and Charlton, P.: Carbon dioxide, water and energy fluxes of irrigated broad-acre crops in an Australian semi-arid climate zone, Environ. Earth Sci., 73, 449–465, https://doi.org/10.1007/s12665-014-3547-4, 2015.

Wang, C.-Y., Wang, J.-N., Wang, X.-F., Luo, D.-L., Wei, Y.-Q., Cui, X., Wu, N., and Bagaria, P.: Phenological Changes in Alpine Grasslands and Their Influencing Factors in Seasonally Frozen Ground Regions Across the Three Parallel Rivers Region, Qinghai-Tibet Plateau, Front. Earth Sci., 9, 797928, https://doi.org/10.3389/feart.2021.797928, 2022.

Wang, S., Grant, R., Verseghy, D., and Black, T.: Modelling plant carbon and nitrogen dynamics of a boreal aspen forest in CLASS—the Canadian Land Surface Scheme, Ecol. Model., 142, 135–154, https://doi.org/10.1016/S0304-3800(01)00284-8, 2001.

Wang, Y., Xiao, J., Ma, Y., Luo, Y., Hu, Z., Li, F., Li, Y., Gu, L., Li, Z., and Yuan, L.: Carbon fluxes and environmental controls across different alpine grassland types on the Tibetan Plateau, Agr. Forest Meteorol., 311, 108694, https://doi.org/10.1016/j.agrformet.2021.108694, 2021.

Wang, Y., Yao, G., Zuo, Y., and Wu, Q.: Implications of global carbon governance for corporate carbon emissions reduction, Front. Environ. Sci., 11, 1071658, https://doi.org/10.3389/fenvs.2023.1071658, 2023a.

Wang, Y., Sun, Y., Chen, Y., Wu, C., Huang, C., Li, C., and Tang, X.: Non-linear correlations exist between solar-induced chlorophyll fluorescence and canopy photosynthesis in a subtropical evergreen forest in Southwest China, Ecol. Indic., 157, 111311, https://doi.org/10.1016/j.ecolind.2023.111311, 2023b.

Wang, Y., Xiao, J., Ma, Y., Ding, J., Chen, X., Ding, Z., and Luo, Y.: Persistent and enhanced carbon sequestration capacity of alpine grasslands on Earth's Third Pole, Sci. Adv., 9, eade6875, https://doi.org/10.1126/sciadv.ade6875, 2023c.

Wang, Z. Y., Li, Z. Y., Dong, S. K., Fu, M. L., Li, Y. S., Li, S. M., Wu, S. N., Ma, C. H., Ma, T. X., and Cao, Y.: Evolution of ecological patterns and its driving factors on Qinghai-Tibet Plateau over the past 40 years, Acta Ecol. Sin., 42, 8941–8952, https://doi.org/10.5846/stxb202204191060, 2022 (in Chinese).

Wehr, R., Munger, J. W., McManus, J. B., Nelson, D. D., Zahniser, M. S., Davidson, E. A., Wofsy, S. C., and Saleska, S. R.: Seasonality of temperate forest photosynthesis and daytime respiration, Nature, 534, 680–683, https://doi.org/10.1038/nature17966, 2016.

World Meteorological Organization: 2019 concludes a decade of exceptional global heat and high-impactweather, https://public.wmo.intlen/media/press-release/2019-concludes-decade-of-exceptional-global-heat-and-high-impact-weather (last access: 5 March 2024), 2019.

Wu, T., Ma, W., Wu, X., Li, R., Qiao, Y., Li, X., Yue, G., Zhu, X., and Ni, J.: Weakening of carbon sink on the Qinghai–Tibet Plateau, Geoderma, 412, 115707, https://doi.org/10.1016/j.geoderma.2022.115707, 2022.

Yasin, A., Niu, B., Chen, Z., Hu, Y., Yang, X., Li, Y., Zhang, G., Li, F., and Hou, W.: Effect of warming on the carbon flux of the alpine wetland on the Qinghai-Tibet Plateau, Front. Earth Sci., 10, 935641, https://doi.org/10.3389/feart.2022.935641, 2022.

Yu, G. and Sun, X.: Principles of flux measurement in terrestrial ecosystem, Beijing: Higher Education Press, ISBN 978-7-04-046012-4, 2006 (in Chinese).

Yu, Y.: Double-order system construction of China's climate change legislation under the dual carbon goals, China Population Resources and Environment, 32, 89–96, https://doi.org/10.12062/cpre.20211120, 2022 (in Chinese).

Zemin, Z., Fenggui, L., Qiong, C., Xingsheng, X., and Qiang, Z.: Spatial Prediction of Potential Property Loss by Geological Hazards based on Random Forest–A Case Study of Chamdo, Tibet, Plateau Science Research, 7, 21–30, https://doi.org/10.16249/j.cnki.2096-4617.2023.02.003, 2023.

Zhang, J., Lin, H., Li, S., Yang, E., Ding, Y., Bai, Y., and Zhou, Y.: Accurate gas extraction (AGE) under the dual-carbon background: Green low-carbon development pathway and prospect, J. Clean. Prod., 377, 134372, https://doi.org/10.1016/j.jclepro.2022.134372, 2022.

Zhang, Y., Zhu, W., Sun, X., and Hu, Z.: Carbon dioxide flux characteristics in an Abies fabri mature forest on Gongga Mountain, Sichuan, China, Acta Ecol. Sin., 38, 6125–6135, https://doi.org/10.5846/stxb201709051599, 2018 (in Chinese).